

## Role of laser-pulse duration in the neutron yield of deuterium cluster targets

K. W. Madison,<sup>1</sup> P. K. Patel,<sup>2</sup> M. Allen,<sup>3</sup> D. Price,<sup>2</sup> R. Fitzpatrick,<sup>1</sup> and T. Ditmire<sup>1</sup>

<sup>1</sup>*Department of Physics, The University of Texas at Austin, Austin, Texas 78712, USA*

<sup>2</sup>*Physics and Advanced Technology Directorate, Lawrence Livermore National Laboratory, Livermore, California 94550, USA*

<sup>3</sup>*Department of Nuclear Engineering, University of California at Berkeley, Berkeley, California 94720, USA*

(Received 14 October 2002; revised manuscript received 25 August 2004; published 18 November 2004)

We present an experimental and computational study of the ion and fusion neutron yields from explosions of deuterium clusters irradiated with 100-TW laser pulses. We find that the cluster explosion energy and resultant fusion yield are sensitive to the laser pulse rise time as determined by the pulse duration for a fixed envelope shape. Our experimental observations are consistent with the results of particle simulations of the laser-cluster interaction which show that the explosion energies of the clusters are determined by a single parameter: the ratio of the cluster ionization time to its intrinsic expansion time. This competition of time scales sets a fundamental constraint on the ion emission and resultant neutron yield performance of these targets as a function of laser-pulse duration.

DOI: 10.1103/PhysRevA.70.053201

PACS number(s): 36.40.Vz, 36.40.Gk, 52.50.Jm, 52.38.Ph

The interaction of intense, ultrashort pulsed lasers with nanometer sized clusters is distinct from gaseous targets of the same composition and average density. For gases containing aggregates of atoms, the clustered ion distribution allows for local electrostatic charging and collective effects such as enhanced electron-ion scattering and inverse bremsstrahlung heating which together greatly increase the laser absorption and produce hot electrons, high energy, and highly charged ion fragments [1–4]. By irradiating deuterium [5,6] or deuterium rich clusters [7,8], nuclear fusion reactions can result, since the deuterium ions attain multi-kilovolt energies from the cluster explosions. In addition to serving as a nonperturbing, *in situ* probe of the relative ion-ion motion produced by the cluster explosions, this fusion source is also

of interest as an ultrafast, pulsed neutron emitter for time resolved material damage studies.

As discussed by Perkins *et al.*, developing such laser driven micro neutron sources suitable for fusion materials testing at high neutron fluence requires the achievement of high neutron yield but would provide a cost effective pure DD or DT fusion neutron source [9]. Table I lists a variety of candidate laser driven sources categorized by target composition. Compared with conventional beam target neutron sources, these sources with small target volumes and laser heat removal by sacrificial vaporization allow close coupling of irradiation specimens resulting in high point neutron fluxes with a pure DD or DT fusion spectrum at low power and low cost. In contrast to inertial confinement fusion (ICF),

TABLE I. Table-top and medium scale laser driven fusion neutron sources.

Reference	Target	Neutron yield (into $4\pi$ )	Laser-pulse parameters			
			Energy (J)	Duration	$\lambda$ ( $\mu\text{m}$ )	$I_{\text{peak}}$ ( $\text{W}/\text{cm}^2$ )
[11]	$\text{C}_8\text{D}_8$ and $\text{D}_2$ solid	$7 \times 10^7$	20	1.3 ps	1.054	$10^{19}$
[12]	$\text{C}_2\text{D}_4$ solid	$1 \times 10^2$	0.2	160 fs	0.79	$10^{18}$
[13]	$\text{CD}_2$ solid	$1 \times 10^7$	7.0	0.3 ps	0.529	$3.5 \times 10^{19}$
[14]	$\text{CD}_2$ solid	$1 \times 10^4$	0.3	0.05 ps	0.8	$2 \times 10^{18}$
[15]	$\text{C}_8\text{D}_8$ solid	$9 \times 10^5$	50	500 fs	1.054	$2 \times 10^{19}$
[16]	$\text{CD}_2$ solid	$5 \times 10^4$	1.5	1.5 ps	1.055	$3 \times 10^{17}$
[17]	$\text{D}_2$ gas	$1 \times 10^6$	62	1 ps	1.05	$2 \times 10^{19}$
[5]	$\text{D}_2$ clusters	$1 \times 10^4$	0.12	35 fs	0.82	$2 \times 10^{16}$
[6]	$\text{D}_2$ clusters	$2 \times 10^6$	10	100 fs	0.8	$2 \times 10^{20}$
[7]	$\text{CD}_4$ clusters	$7 \times 10^3$	0.8	35 fs	0.82	$2 \times 10^{17}$
[8]	$\text{CD}_4$ clusters	$1 \times 10^5$	2.5	100 fs	0.8	$4 \times 10^{19}$

where, for example,  $5 \times 10^9$  DD fusion neutrons were produced from an ICF implosion by the Nova laser using 30 kJ of light [10], the laser driven neutron sources considered here do not require a large scale laser facility and may offer an adequate neutron flux for materials studies at a fraction of the pulse energy and at much higher repetition rates. Nonetheless, in order to reach the required fluxes for this application, the yield of these sources must be increased by another two orders of magnitude, to  $10^9$  neutrons per shot. This article provides a detailed characterization and analysis of the fusion neutron yield dependence on laser parameters for deuterated cluster targets, and demonstrates that  $10^9$  neutrons per shot is possible with pulse energies below 500 J.

The purpose and motivation of this work was to study the laser-cluster interaction in the untested regime of peak laser intensities above  $10^{18}$  W/cm<sup>2</sup> and to fully characterize the resultant fusion yield as a function of the laser and target parameters in order to determine the optimum conditions and ultimate expected performance of these cluster fusion neutron sources on various state-of-the-art laser facilities. A related and hitherto unexplained feature observed in all cluster-fusion experiments performed to date is that the neutron yield follows a quadratic power law dependence on pulse energy. In this article, we explain the observed fusion dependencies and report on the critical role that the laser field rise time, as determined by the pulse duration for a fixed envelope shape, has on the ion energies and resultant fusion yield of a deuterium cluster target. In particular, we find that for intensities above  $10^{18}$  W/cm<sup>2</sup> the ion energies are only weakly modified by changes in the pulse energy and therefore peak laser intensity at a given pulse duration. The result is that for a fixed pulse duration, the fusion yield dependence on pulse energy is determined primarily by the plasma volume scaling. It is well known that at much lower intensities, the cluster explosions are strongly intensity dependent since the larger aggregates in the ensemble of clusters will not undergo a complete Coulomb explosion, truncating the resultant ion distribution, and limiting the fusion yield [18]. In contrast to the observed insensitivity to changes in the pulse energy and therefore peak intensity, the ion energies are dependent on the pulse rise time, as determined by the pulse duration. While electron heating [19] and plasmon enhanced ionization [28] in cluster targets are also strongly dependent on the laser pulse duration, the phenomenon studied here is not a resonant effect but rather involves a basic competition of time scales. Using an analytic model and a simple particle simulation of the laser induced cluster explosions, we find that our data are consistent with an ensemble of clusters undergoing a pure Coulomb explosion for which the efficacy is determined by a single parameter: the ratio of the cluster ionization time to its intrinsic expansion time. This effect is related to the observation that nuclear motion can occur during laser ionization of single molecules and modify their fragmentation pattern [20], and it sets fundamental constraints on the performance of these fusion neutron sources. In particular, it is shown that for peak laser fields which exceed the space charge forces of a given cluster, the explosion efficiency for a deuterium cluster is only marginally improved for reductions in the pulse duration below 200 fs.

In our experiments, a dense plume of deuterium clusters

was produced by expansion of the gas from a high pressure (1000 psi), cryogenically cooled (114 K) reservoir into a vacuum through a 750- $\mu$ m orifice and a conical nozzle. Two different types of nozzles were used to obtain either a sonic (with a cone opening angle of 76° and length of 1 mm) or a supersonic (with a cone opening angle of 20° and length of 12.5 mm) expansion. The atomic density of the cluster plume (2.5 mm below the nozzle opening) was determined from an *in situ*, transverse, interferometric image of the plasma filament [21] and found to reach a peak density of  $6(\pm 2) \times 10^{18}$  cm<sup>-3</sup> and  $7(\pm 4) \times 10^{18}$  cm<sup>-3</sup> for the sonic and supersonic nozzles, respectively.

The gas plume was irradiated by a single pulse of 800-nm light from the LLNL (Lawrence Livermore National Laboratory) JanUSP laser [22]. The temporal envelope was Gaussian [ $I(t) = I_{\text{peak}} e^{-(t/t_p)^2}$ ] and the pulse had a contrast of better than  $10^{-7}$ . The maximum pulse energy was 10 J and we varied the full width at half maximum duration ( $T_{\text{FWHM}} = 2t_p \sqrt{\ln 2}$ ) of the compressed pulse from 100 fs to 1 ps by varying the grating spacing in the pulse compressor. After recompression, this pulse was focused into the gas plume by a 0.3-m focal length off-axis parabolic mirror producing a vacuum focal spot diameter of  $5 \mu$   $\mu$ m containing 30% of the total laser energy. This configuration yielded a peak intensity of  $2 \times 10^{20}$  W/cm<sup>2</sup> in vacuum with a prepulse intensity of  $10^{13}$  W/cm<sup>2</sup>, well below the ionization threshold of deuterium.

In order to characterize the energy distribution of the deuterium ions produced, we employed two Faraday cups. Cup A was 0.52 m behind the laser focus and aligned 15° from the laser propagation axis  $\mathbf{k}$ , and cup B was 0.36 m from the focus and aligned 15° from the polarization axis and 90° from the first cup. Each detector was composed of a grounded screen and body followed by the electrode which was negatively biased (-400 V) to reject electrons accompanying the ions. A typical ion time-of-flight signal is shown in Fig. 1, and possesses three distinct features: an initial 100-ns-wide photoelectron current spike from photons and energetic electrons (greater than 400 eV) ejecting secondary electrons from the negatively biased electrode, an ion current peak between 200 and 800 ns due to the arrival of energetic deuterium ions generated in the cluster explosions, and a large ion current starting after 2  $\mu$ s due to the arrival of slower deuterium ions whose energy is consistent with the breakout velocity of a Taylor-Sedov blast wave launched in the neutral plume by the filament expansion [21]. For each shot, the average ion energy  $\bar{E}_i$  and ion yield  $N_i$  were determined from the energetic ion peak. Although the ions originate from the explosions of an ensemble of clusters with a distribution of cluster sizes, the energy distribution is well characterized by a Maxwellian distribution, and the resulting fit is shown in Fig. 1 by the thin solid line.

To determine the fusion yield, we counted the number of 2.45-MeV neutrons emitted with an array of plastic scintillating detectors. The characteristic deuterium fusion energy of the neutrons was verified by measuring their flight time of 46 ns/m. The fusion neutron yield from an irradiated cluster plume formed in a sonic expansion of deuterium gas was measured as a function of pulse energy for two different

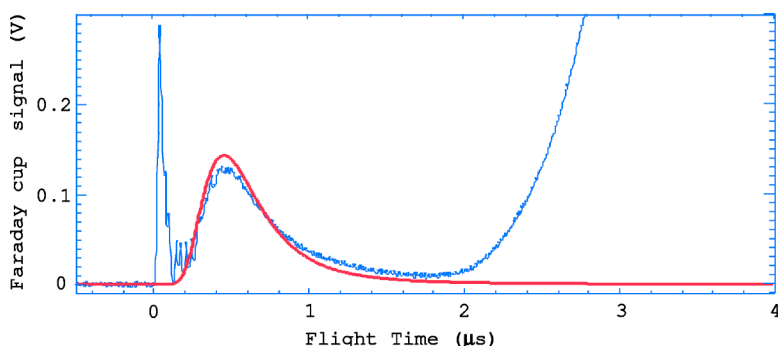


FIG. 1. Time-of-flight (TOF) ion current captured on Faraday cup A from a supersonic cluster plasma irradiated by a 100-fs pulse of energy 5.4 J. The part of this current corresponding to the energetic deuterium ions generated in the cluster explosions is fitted to a Maxwellian distribution (thin solid line) providing the number and average energy in this group.

pulse durations, 100 fs and 1 ps, and is shown in Fig. 2. The error bars represent the (Poissonian) statistical uncertainty associated with the number of neutrons counted in a detector for each shot. The yield is well characterized by a power law dependence on pulse energy,  $Y=QE^\alpha$ , where  $Q=1.32 \times 10^4$  and  $\alpha=2.15$  and  $Q=1.43 \times 10^3$  and  $\alpha=2.29$  for the 100 fs and 1 ps shots, respectively. Quite remarkably, this roughly quadratic dependence of the yield on pulse energy is robust over two orders of magnitude corresponding to two orders of magnitude in vacuum peak laser intensity, from  $2 \times 10^{20}$  to  $2 \times 10^{18}$  W/cm<sup>2</sup> for the 100 fs data. A very similar quadratic dependence was found previously with  $Q=3.24 \times 10^6$  and  $\alpha=2.29$  for shots on the LLNL Falcon laser for pulse energies between 10 and 120 mJ [23]. For that experiment, the pulse duration was 35 fs and the vacuum focal spot size was 100  $\mu\text{m}$  yielding intensities between  $2 \times 10^{16}$  and  $2 \times 10^{17}$  W/cm<sup>2</sup>. Therefore this quadratic yield dependence on pulse energy is evidently independent of pulse duration, peak laser intensity (in the range  $2 \times 10^{16}$  to  $2 \times 10^{20}$  W/cm<sup>2</sup>), and focal geometry. The absolute magnitude of the neutron yield is, however, clearly dependent on the pulse duration. In particular, the yield in our experiments for a fixed geometry is a factor of 8 smaller with

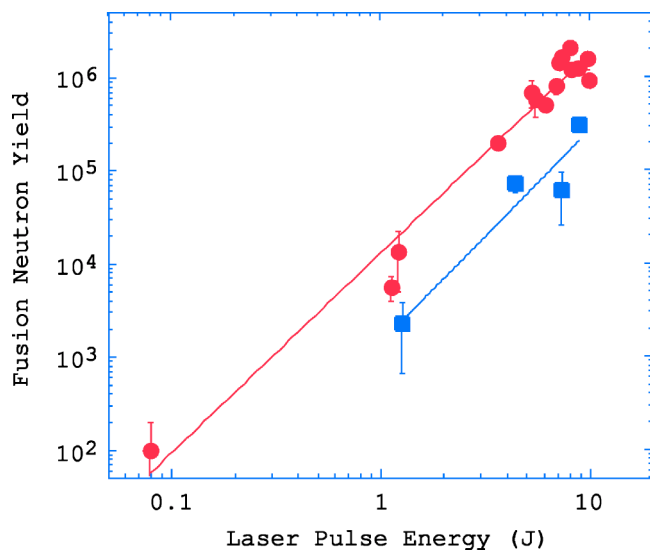


FIG. 2. Fusion neutron yield from exploding deuterium cluster plasmas as a function of pulse energy for two different pulse durations: 1 ps (squares) and 100 fs (circles). The solid lines are the least mean squares fit to a power law dependence of the yield on pulse energy.

1-ps pulses than for 100 fs and is consistent with the predicted reduction in ion energies due to the longer cluster ionization time associated with the longer pulse duration.

It is important to note here that the explosion of a given cluster does not result in any fusion events and only serves to accelerate the constituent ions relative to one another. Only after the ions from neighboring clusters overlap does fusion begin, and this happens more than 50 fs after the ions have been fully accelerated (given the gas density and average cluster size in this experiment). Moreover, the average collision probability of a given ion as it traverses the filament and gas plume is less than  $10^{-8}$ , so the fusion events in this experiment can be viewed as a nonperturbative probe of the effective ion temperature long after the explosion dynamics are complete.

In order to identify the origins of the fusion yield dependence on the laser parameters, it is useful to investigate the ion emission from the plasma as a function of these parameters as well. Figure 3 shows, as a function of the pulse energy, the total yield and average energy of the energetic ion component emitted from irradiated deuterium clusters formed in a supersonic expansion. The average cluster size was measured by Rayleigh scattering to be (6 nm radius) a factor of 1.2 larger than that produced in the sonic expansion (5 nm). In addition to the ion yield, the fusion neutron yield expected from the measured ion spectra is calculated and shown along with the measured neutron flux for each shot. The points below 0.5 J are the average of ten or more shots while those above 0.5 J are the measurements from single laser shots. The dependence of the average energy and ion yield on pulse energy is fit by a power law (lines), and the average energy is given by  $\bar{E}_i \sim 9.4E^{0.18}$  keV for cup A and  $\bar{E}_i \sim 11.2E^{0.19}$  keV for cup B, while the total ion yield was, assuming isotropic emission,  $N_i \sim 4.3 \times 10^{14}E^{1.1}$  for cup A and  $N_i \sim 3.4 \times 10^{14}E^{0.94}$  for cup B. Despite the different placement of the two detectors, no major difference in the ion energies was observed, suggesting that the high energy portion of the ion emission was, for the most part, unmodified by inelastic collisions with the unionized part of the plume and also roughly isotropic. The ion energy measured along  $\mathbf{k}$  (by cup A) was slightly lower (by 15%) than that measured perpendicular to  $\mathbf{k}$ , and this difference is accounted for in the expected fusion yield in Fig. 2. We note that this slight anisotropy seems consistent with recent measurements of exploding argon clusters [25].

Although the energy and therefore intensity were varied over more than two decades (from 50 mJ to 6.3 J corre-

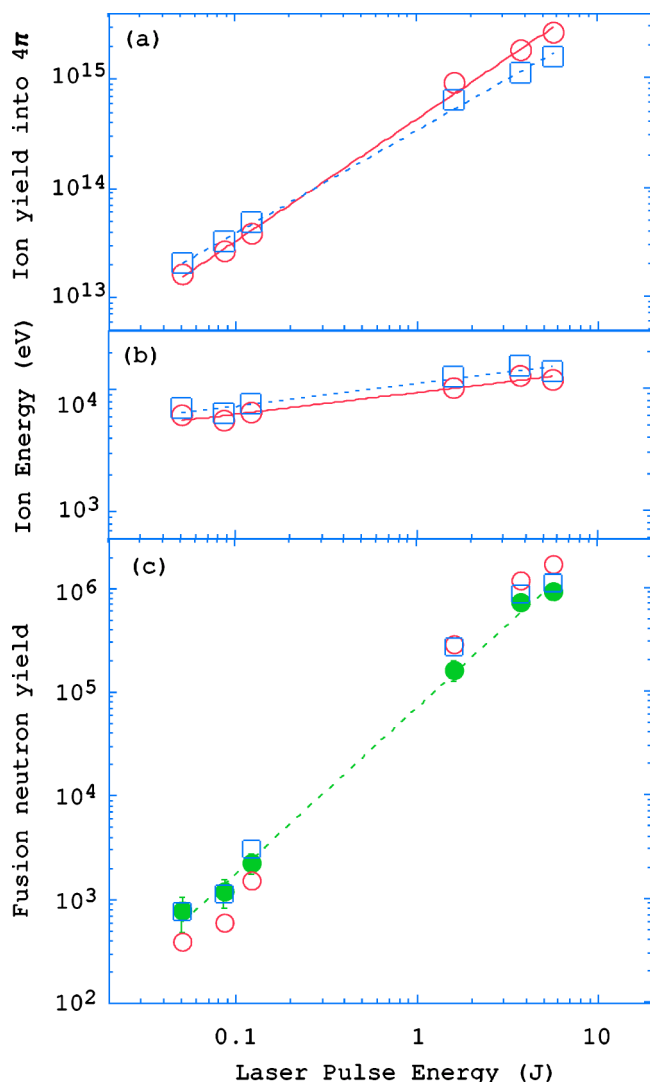


FIG. 3. Ion yield (a), average ion energy (b), and fusion neutron yield (c) as a function of laser energy for a 100 fs pulse duration. The ion yield and energies as well as the expected fusion neutron yield were determined from the two Faraday cup signals: cup A (open circles) and cup B (open squares). The measured fusion neutron yield at each energy is also shown (filled circles) and fitted to a power law dependence (dotted line) with  $Y = QE^\alpha$ , where  $Q = 7.1 \times 10^4$  and  $\alpha = 1.6$ .

sponding to peak vacuum intensities of  $1.0 \times 10^{18}$  and  $1.2 \times 10^{20}$  W/cm<sup>2</sup>, respectively), the average ion energy varied by little more than a factor of 2. This observed insensitivity to variations of the input energy at a fixed pulse duration suggests that the cluster explosion mechanism is unaffected by the final peak laser intensity even when the laser field is large enough to induce relativistic electron motion. Furthermore, such an observation is indicative that the cluster explosion occurs before the peak field is attained.

The expected fusion yield generated inside the plasma filament was estimated from the expression

$$Y \approx \frac{\tau_d}{2} \int n_D^2 \langle \sigma v \rangle dV, \quad (1)$$

where  $\tau_d$  is the disassembly time of the filament,  $n_D$  is the

average deuterium density (measured *in situ*),  $\langle \sigma v \rangle$  is the velocity averaged fusion cross section (calculated from the measured ion energies), and the integration is over the initial volume of the plasma. Since the measured ion density is approximately uniform over the interaction region, the initial plasma volume is simply  $V = N_i / n_D$ . The plasma disassembly time will depend on the volume and shape of the plasma and on the average ion velocity, which for a Maxwellian distribution is  $\bar{v} = \sqrt{16\bar{E}_i / 3\pi m_{\text{ion}}}$ . Assuming the shape of the plasma generated does not change with increasing pulse energy, we can write that  $\tau_d = \gamma V^{1/3} / \bar{v}$  where the constant factor  $\gamma$  is a unitless quantity which accounts for the plasma geometry and is of order 1. In this case, Eq. (1) reduces to

$$Y \approx \frac{\gamma}{2} n_D^{2/3} \sqrt{\frac{3\pi m_{\text{ion}}}{16 \text{ (eV)}}} \left( \frac{N_i^{4/3}}{\bar{E}_i^{1/2}} \langle \sigma v \rangle \right), \quad (2)$$

where  $\bar{E}_i$  is now in units of eV. For a fixed geometry and constant density, the yield dependence on the measured ion emission is transparent and described by the quantity in parenthesis. In Fig. 3(c) the estimated fusion neutron yield was calculated assuming the parameter  $\gamma = 1.0$ .

Since for these data  $N_i$  varied linearly with the pulse energy and  $\bar{E}_i \propto E^{0.2}$  (so that  $\langle \sigma v \rangle / \bar{E}_i^{1/2}$  scaled as  $E^{0.4}$ ), the expected yield follows closely the actual yield dependence [shown by the dotted line in Fig. 3(c)] for these shots of  $E^{1.6}$ .

Without performing a detailed calculation of the depletion of the laser pulse as it propagates through the cluster medium, the exact geometry (length and radial profile) of the plasma filament cannot be inferred. However, since it is that part of the plume illuminated above the ionization threshold which defines the relevant plasma volume, one can assume that the shape of the plasma volume grows with increasing pulse energy and at fixed pulse duration in the same way as does an isointensity contour of a paraxial beam propagating in a homogeneous medium. From previous observations of self-focusing and beam filamentation in cluster plumes [26], we know this assumption is not ideal; however, the agreement between the measured and expected yield is good over the entire domain studied, supporting our assumption that these and other possible variations in propagation do not significantly alter the relevant plasma characteristics (geometry and density) as the pulse energy is varied. In addition, this agreement between the two sets of measurements provides a strict self-consistency check on the accuracy and validity of each.

It is evident that the roughly quadratic dependence of the neutron yield on pulse energy results from the fact that the ion number yield scales linearly with the pulse energy, and therefore the fusion yield should scale at least as fast as  $E^{4/3}$ . The minor variation in ion average energy with pulse energy does contribute to the yield scaling but only as  $E^{0.4}$  in this range. Over the two fold increase in ion energy the fusion reactivity increases by a factor of 10 (as the effective ion temperature increases from  $k_B T = 2/3 \bar{E}_i = 4$  keV for 50-mJ pulses to 9.3 keV for 5-J pulses), but at the same time, the plasma disassembly time (for a fixed volume) drops by a factor of 1.4. These two competing factors only increase the

total fusion yield by a factor of 6 or 7, a much less significant increase compared to the factor of almost 500 in yield due to the increase in plasma volume. The fact that the yield scaling is slightly higher,  $E^{2.2}$ , in the case of clusters produced in a sonic expansion (see Fig. 2), probably results from the fact that the gas density and cluster size vary more strongly with the distance from the jet center. In this case, larger pulse energies penetrate to regions of higher density and larger clusters where the resultant fusion reactivity is consequently larger.

From Fig. 3(b) it is clear that the cluster explosion energy is rather insensitive to changes in the peak laser intensity above  $10^{18}$  W/cm<sup>2</sup> (changing by a factor of 2 with a change of 100 in peak intensity) while strongly dependent on the pulse duration, as evident from the shift in the overall fusion yield for different pulse durations. In order to understand this aspect of deuterium cluster explosions, we have performed molecular dynamics simulations of the explosions of  $N$ -ion clusters, where the atomic ionization of the constituents is calculated from the Ammosov-Delone-Krainov (ADK) formula for tunneling ionization [27], and the motion of the resulting plasma is calculated from classical, charged-particle dynamics in the self-consistent field. These particle simulations are similar to the calculations of Teuber *et al.* [28] who considered metallic clusters and Last and Jortner who considered heteronuclear clusters [24]. Unlike in the work of Teuber *et al.*, the ionization dynamics here are included in the simulation and not assumed to be spatially uniform across the cluster nor assumed to follow an *ad hoc* time dependence.

The simulations performed for various pulse durations and peak laser intensities (where we assume a temporal Gaussian pulse shape) provide the time scale  $t_{\text{ion}}$  over which the cluster is stripped of 63% of its electrons, and the final average kinetic energy of the ions  $\bar{E}_i$  obtained in the explosion. Both quantities are scaled by the characteristic time  $t_{\text{exp}}$  and energy  $E_{\text{exp}}$  of the Coulomb expansion, where  $E_{\text{exp}} = (3m_{\text{ion}}/5)(a_0/t_{\text{exp}})^2$ ,  $t_{\text{exp}} = \sqrt{3m_{\text{ion}}\epsilon_0/e^2n_0}$ ,  $m_{\text{ion}}$  is the ion mass,  $\epsilon_0$  is the electric permittivity of free space,  $e$  is the average charge state per ion within the cluster,  $n_0 \sim 3 \times 10^{22}$  cm<sup>-3</sup> is the ion density inside the cluster, and  $a_0$  is the initial cluster radius.

The ionization probability of each atom within the cluster was calculated using the ADK rate induced by the electric field of the laser, and the electrons were assumed to vanish forever from the cluster as soon as they were extracted. This simplification was made to reduce the computational cost of the simulations without changing the character of the cluster explosions, but it may nevertheless affect the ionization rate. By neglecting the presence of the free electrons, electron-ion collisions are neglected which could also modify the cluster ionization rate and to some degree the cluster expansion dynamics.

In Fig. 4 the results of the simulation are shown for various cluster sizes and peak laser intensities where the pulse duration was scanned from 25 to 3200 fs (doubling between each data set). The results are, for the cases studied, independent of cluster size and lie on the same universal curve of explosion energy (normalized by  $E_{\text{exp}}$ ) versus ion-

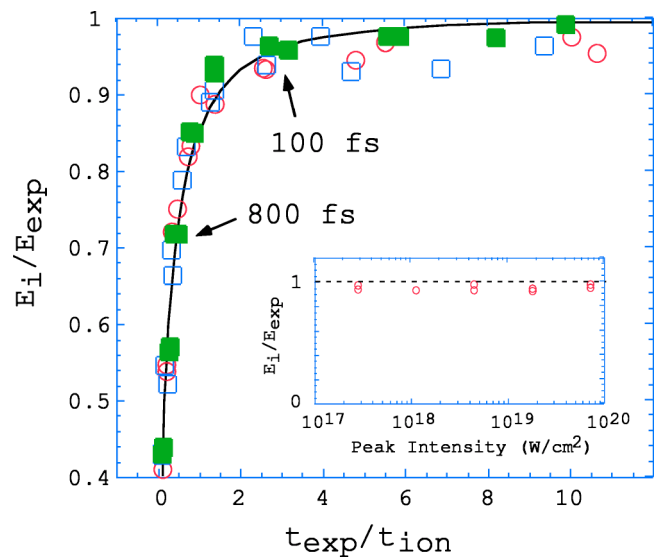


FIG. 4. Average ion energy from a cluster explosion plotted against the ratio  $g = t_{\text{exp}}/t_{\text{ion}}$ . The cluster expansion time  $t_{\text{exp}} \sim 10.7$  fs, and the cluster ionization time was calculated at various pulse durations between 25 and 3200 fs (doubling between each data set—the results at 100 fs and 800 fs are marked) for clusters of sizes  $N=100$  (empty circles and squares) and  $N=1000$  (filled squares). The peak laser intensities were  $2.8 \times 10^{17}$  (circles) and  $1.12 \times 10^{18}$  W/cm<sup>2</sup> (squares). The inset shows a calculation of the final explosion energy for a cluster of size  $N=100$ , a pulse duration of 100 fs, and various peak laser intensities.

ization time. The solid black line is the numerical solution of a simple fluid model of a self-similar, purely radial cluster expansion assuming a uniform mass and charge density, and an average ionization state for the entire cluster which varies as  $\langle q \rangle = 1 - e^{-t/t_{\text{ion}}}$ , where the value for the ionization time is taken from the simulation. In this simple model, the equation of motion for the cluster radius is given by

$$\frac{d^2\rho}{d\tau^2} = \frac{(1 - e^{-g\tau})^2}{\rho^2}, \quad (3)$$

where  $\rho = r(t)/r(0)$  is the normalized cluster radius,  $\tau = t/t_{\text{exp}}$  is the normalized time, and  $g = t_{\text{exp}}/t_{\text{ion}}$  is the ratio of the expansion time to the ionization time. In the limit of instantaneous ionization ( $g \rightarrow \infty$ ), Eq. (3) can be integrated [18] to give the normalized kinetic energy as a function of the normalized radius

$$\frac{1}{2} \left( \frac{d\rho}{d\tau} \right)^2 = 1 - \frac{1}{\rho}. \quad (4)$$

In this limit ( $g \rightarrow \infty$ ), the final ( $\tau \rightarrow \infty$ ), normalized kinetic energy (of the cluster expansion) is one, corresponding to an average kinetic energy for the ejected ions of  $E_{\text{exp}}$ . We can, in general, seek a solution to the final normalized kinetic energy as a function of  $g$ , and although we have found no analytic solution to (3), the following function closely approximates the numerical solutions shown in Fig. 4:

$$F(g) = \lim_{\tau \rightarrow \infty} \frac{1}{2} \left( \frac{d\rho}{d\tau} \right)^2 \approx 1 - e^{-2\sqrt{g}}. \quad (5)$$

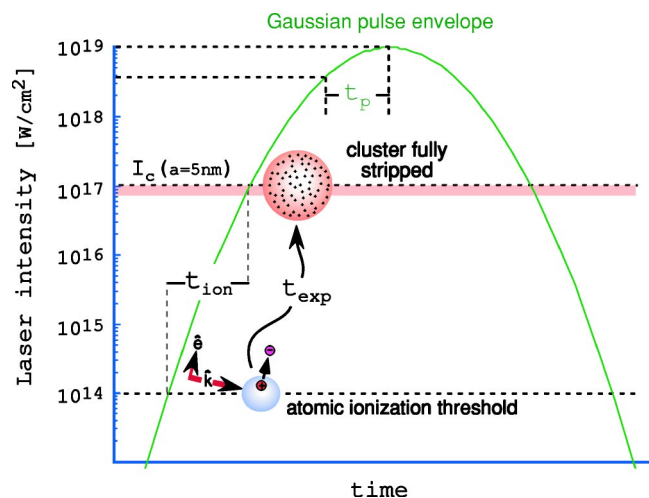


FIG. 5. Schematic of cluster ionization and expansion dynamics during the laser pulse. The ionization time  $t_{\text{ion}}$  is determined by the time required for the laser intensity to rise from the first threshold, at which atomic ionization begins, to the second threshold, at which the electric field of the laser exceeds the threshold for complete ion charge uncovering (approximately when the laser electric field exceeds the space charge electric field of the fully stripped cluster) [18]. The second threshold, which is shown for a cluster of radius  $a=5$  nm, depends on the size and density of the cluster and will fall from its initial value as the cluster expands. Because of the finite duration of the cluster ionization time, the cluster will explode more slowly than its characteristic expansion time  $t_{\text{exp}}$  resulting in a final kinetic energy below the characteristic energy  $E_{\text{exp}}$  by the factor  $1/F(g)$ .

In the inset of Fig. 4, the cluster explosion energy is shown at various peak intensities for a fixed pulse duration of 100 fs. Consistent with the experimental observations, the explosion energy is found to be almost completely independent of the peak laser intensity for 100 fs pulses.

In the simulation, as illustrated in Fig. 5, electron extraction from the cluster is observed to begin at the tunneling ionization threshold ( $\sim 10^{14}$  W/cm<sup>2</sup>) and end once the laser field exceeds the threshold for complete ion charge uncovering [18] (approximately when the laser field exceeds the space charge electric field of the fully stripped cluster—e.g.,  $I > 2.7 \times 10^{16}$  W/cm<sup>2</sup> for  $N=1000$  or  $a=2$  nm). Of course, the second threshold, which is shown in Fig. 5 for a cluster of radius  $a=5$  nm, depends on the size and density of the cluster and it will fall from its initial value as the cluster expands. In any event, because of the finite duration of the cluster ionization time, the cluster will explode more slowly

than its characteristic expansion time  $t_{\text{exp}}$  resulting in a final kinetic energy below the characteristic energy  $E_{\text{exp}}$  by the factor  $1/F(g)$ .

The observed insensitivity to variations of the intensity at a fixed pulse duration can therefore be understood in the following way. If the peak intensity lies far above the second threshold, changes in the final laser intensity only affect logarithmically the ionization duration (by changing the average slope of the envelope between the two thresholds—see Fig. 5) and these logarithmically small changes in  $g$ , about the value  $g=3$  where  $F(g)$  is relatively flat, have little effect on the final explosion energy.

For a pulse duration of 100 fs, the ionization time was  $t_{\text{ion}} \sim 5$  fs and the average ion energy was 0.96 of  $E_{\text{exp}}$ , while for a pulse duration of 1 ps, the ionization time was  $t_{\text{ion}} \sim 33$  fs and the average ion energy was 0.67 of  $E_{\text{exp}}$ , a reduction of 30% in energy. Under the same experimental conditions as for the data presented in Fig. 2, the average ion energy was measured to be  $\bar{E}_i \approx 4$  keV for an incident pulse of 1 J and 100 fs. If we assume the explosion energies were lower by 30% for the 1-ps shots, then the plasma reactivity would have been a factor of 4.3 lower and close to the measured factor of 8 reduction in fusion yield.

A similar reduction in the ion energies with increasing pulse duration was previously observed in explosions of metallic clusters; however, also in that case the maximum charge state attained by the ions was observed to exhibit a resonant enhancement as a function of pulse duration [28]. In that work the ion kinetic energies are observed to be unaffected by the additional cluster charging from plasmon enhanced ionization, and the authors conclude that the initial ionization dynamics during the cluster expansion are what determine the final kinetic energies. In a similar fashion, the explosion dynamics of deuterium clusters in these experiments is also determined by the ionization dynamics and is consistent with a single-parameter, Coulomb-explosion model where the efficacy of the explosion is determined by the ratio of the cluster ionization time to the intrinsic expansion time. The identification of this fundamental time scale and its role in cluster explosions explains the observation that the ion energies are almost completely independent of the peak laser intensity and, by consequence, why the observed fusion yield scaling is primarily a plasma volume effect. It is clear from Fig. 4 that, as a result of the rollover, there exists an intrinsic constraint on the performance of these fusion neutron sources, and the explosion efficiency is only marginally improved for reductions of the pulse duration below 200 fs.

- [1] A. McPherson, B. D. Thompson, A. B. Borisov, K. Boyer, and C. K. Rhodes, *Nature (London)* **370**, 631 (1994).
- [2] E. M. Snyder, S. Wei, J. Purnell, S. A. Buzza, and A. W. Castleman, Jr., *Chem. Phys. Lett.* **248**, 1 (1996).
- [3] T. Ditmire, J. W. G. Tisch, E. Springate, M. B. Mason, N. Hay, R. A. Smith, J. Marangos, and M. H. R. Hutchinson, *Nature*

(London) **386**, 54 (1997).

- [4] M. Lezius, S. Dobosz, D. Normand, and M. Schmidt, *Phys. Rev. Lett.* **80**, 261 (1998).
- [5] T. Ditmire, J. Zweiback, V. P. Yanovsky, T. E. Cowan, G. Hays, and K. B. Wharton, *Nature (London)* **398**, 489 (1999).
- [6] K. W. Madison, P. K. Patel, M. Allen, D. Price, and T. Ditmire,

- J. Opt. Soc. Am. B **20**, 113 (2003).
- [7] G. Grillon, Ph. Balcou, J.-P. Chambaret, D. Hulin, J. Martino, S. Moustazis, L. Notebaert, M. Pittman, Th. Pussieux, A. Rousse, J- Ph. Rousseau, S. Sebban, O. Sublemontier, and M. Schmidt, Phys. Rev. Lett. **89**, 065005 (2002).
- [8] K. W. Madison, P. K. Patel, D. Price, A. Edens, M. Allen, T. E. Cowan, J. Zweiback, and T. Ditmire, Phys. Plasmas **11**, 270 (2004).
- [9] L. J. Perkins, B. G. Logan, M. D. Rosen, M. D. Perry, T. Diaz de la Rubia, N. M. Ghoniem, T. Ditmire, S. Wilkes, and P. T. Springer, Nucl. Fusion **40**, 1 (2000).
- [10] T. R. Dittrich, B. A. Hammel, C. J. Keane, R. McEachern, R. E. Turner, S. W. Haan, and L. J. Suter, Phys. Rev. Lett. **73**, 2324 (1994).
- [11] P. A. Norreys, A. P. Fews, F. N. Beg, A. R. Bell, A. E. Dangor, P. Lee, M. B. Nelson, H. Schmidt, M. Tatarakis, and M. D. Cable, Plasma Phys. Controlled Fusion **40**, 175 (1998).
- [12] G. Pretzler, A. Saemann, A. Pukhov, D. Rudolph, T. Schätz, U. Schramm, P. Thirolf, D. Habs, K. Eidmann, G. D. Tsakiris, J. Meyer-ter-Vehn, and K. J. Witte, Phys. Rev. E **58**, 1165 (1998).
- [13] L. Disdier, J.-P. Garçonnet, G. Malka, and J.-L. Miquel, Phys. Rev. Lett. **82**, 1454 (1999).
- [14] D. Hilscher, O. Berndt, M. Enke, U. Jahnke, P. V. Nickles, H. Ruhl, and W. Sandner, Phys. Rev. E **64**, 016414 (2001).
- [15] N. Izumi, Y. Sentoku, H. Habara, K. Takahashi, F. Ohtani, T. Sonomoto, R. Kodama, T. Norimatsu, H. Fujita, Y. Kitagawa, K. Mima, K. A. Tanaka, and T. Yamanaka, Phys. Rev. E **65**, 036413 (2002).
- [16] V. S. Belyaev, V. I. Vinogradov, A. S. Kurilov, A. P. Matafonov, V. P. Andrianov, G. N. Ignat'ev, A. Ya. Faenov, T. A. Pikuz, I. Yu. Skobelev, A. I. Magunov, S. A. Pikuz, Jr., and B. Yu. Sharkov, JETP **98**, 1133 (2004).
- [17] S. Fritzler, Z. Najmudin, V. Malka, K. Krushelnick, C. Marle, B. Walton, M. S. Wei, R. J. Clarke, and A. E. Dangor, Phys. Rev. Lett. **89**, 165004 (2002).
- [18] P. B. Parks, T. E. Cowan, R. B. Stephens, and E. M. Campbell, Phys. Rev. A **63**, 063203 (2001).
- [19] J. Zweiback, T. Ditmire, and M. D. Perry, Phys. Rev. A **59**, R3166 (1999); L. M. Chen, J. J. Park, K. H. Hong, I. W. Choi, J. L. Kim, J. Zhang, and C. H. Nam, Phys. Plasmas **9**, 3595 (2002); H. M. Milchberg, S. J. McNaught, and E. Parra, Phys. Rev. E **64**, 056402 (2001).
- [20] C. Cornaggia, M. Schmidt, and D. Normand, Phys. Rev. A **51**, 1431 (1995).
- [21] J. Zweiback and T. Ditmire, Phys. Plasmas **8**, 4545 (2001).
- [22] F. G. Patterson, J. Bonlie, D. Price, and B. White, Opt. Lett. **24**, 963 (1999).
- [23] T. Ditmire, J. Zweiback, V. P. Yanovsky, T. E. Cowan, G. Hays, and K. B. Wharton, Phys. Plasmas **7**, 1993 (2000).
- [24] I. Last and J. Jortner, Phys. Rev. Lett. **87**, 033401 (2001).
- [25] V. Kumarappan, M. Krishnamurthy, and D. Mathur, Phys. Rev. Lett. **87**, 085005 (2001).
- [26] I. Alexeev, T. M. Antonsen, K. Y. Kim, and H. M. Milchberg, Phys. Rev. Lett. **90**, 103402 (2003).
- [27] M. V. Ammosov, N. B. Delone, and V. P. Krainov, Sov. Phys. JETP **64**, 1191 (1986).
- [28] S. Teuber, T. Töppner, T. Fennel, J. Tiggesbäumker, and K. H. Meiwes-Broer, Eur. Phys. J. D **16**, 59 (2001).